RSC Advances

ROYAL SOCIETY OF CHEMISTRY

www.rsc.org/advances

RSC Advances

ARTICLE

Effect of aggregation behavior and phenolic hydroxyl group content on the performance of lignosulfonate doped PEDOT as hole extraction layer in polymer solar cells

Received 00th January 20xx,
Accepted 00th January 20xx

DOI: 10.1039/x0xx00000x

www.rsc.org/

NanlongHong,[a,b] Xueqing Qiu*[a,b] Wanyuan Deng,[c] Zhicai He*[c] and Yuan Li*[a,b]

Using lignosulfonate (LS) and alkyl chain-coupled lignosulfonate-based polymer (ALS) as raw material, the aggregation behavior of LS and ALS was investigated, which all showed unique aggregation behavior to form block-like self-assembly for the first time. The aggregation behavior and mechanism of LS and ALS was investigated by SEM, TEM and DLS. T block-like aggregates prepared from ALS (micron size) were larger than that of LS (nano size). The unique aggregates were also further confirmed by XPS, meanwhile, SAXS was applied to explore the regular intrinsic characteristics of the bloc like aggregates. Inspired by the aggregation behavior of LS and ALS, the electron transfer properties of LS and ALS were also studied including electrochemical property and hole mobility measurement. The oxidation peaks at 1.2 V and 1.4 V were observed at the LS and ALS modified electrode, respectively. We studied hole transport property of LS and ALS with space-charge-limited current method (SCLC). The average hole mobilities of 2.95×10^{-6} cm^2 V^{-1} s^{-1} and 3.18×10^{-7} cm^2 V^{-1} s were estimated for LS and ALS, respectively. The above results indicated that LS and ALS are potential water soluble polymeric p-type semiconductors, and the electron transfer property of LS is better than that of ALS. Based on the unique aggregation behavior and hole mobility above which will facilitate charge transport, water soluble PEDOT:LS and PEDOT:ALS were prepared and applied as hole extraction layer (HEL) in polymer solar cells. The PCE decreased with the decrease of phenolic hydroxyl group content (-OH), which suggested that –OH is important for the property of PCE. The application properties were consistent with the results of aggregation behavior and electron transfer properties. The power conversion efficiency (PCE) of 5.19% from PEDOT:LS-1:1 as HTL was achieved with device structure of ITO/HEL/PTB7:PC71BM/Al in our study. Our results showed the phenolic hydroxyl group content and conjugation structure of amorphous LS contribute its promising potential as dopant of semiconductors, such as PEDOT in organic electroni Our result provides a novel perspective for the design of dopant for semiconductive polymer.All in one word, phenolic hydroxyl group of polymer will provide hole transport capability due to its oxidation during device orperation.

Introduction

Self-assembled aggregates from polymer have attracted considerable attention owing to their unique ordered structure, including spheres,[1] wires,[2] sheets,[3] rods,[4] vesicles,[5] and many other complex system such as anisotropic, patterned or hierarchical materials.[6-8] The various structures are central to a range of advanced application nanotechnology.[9-11] In previous work, various of controllable self-assemblies can realized with numerous synthetic polymer with known structure such as poly (styrene sulfonic acid) (PSS)[12] and Poly(N-isopropylacrylamide) (PNI)[13], however, it is relatively challenging to obtain unique self-assembly with amorphous polymer. Recently, we are surprised to find that lignosulfonate (LS) and alkyl chain-coupled lignosulfonate-basedpolymer (ALS from our previous manuscript[14] can form unique block-like self-assembly in selective solvent without help from a foreign interface. To the most of our knowledge, similar self-assembly from water soluble amorphous polymer has been rarely reported, to date.

In our previous work,[14,15] It is well known amorphous lignosulfonate (LS) exist as small aggregate with nano-size in solution. However the unique block-like aggregate from LS in selective solvent is rarely reported and very different with nanospheres of LS. The high value-added application of L motivate is of great importance. We notice an odd chemist that lignin and lignosulfonate will be converted into oxidized state with radicals, which can be detected by electron sp n resonance (ESR).[16-18] Inspired by the unique aggregation behaviour of LS and ALS via its self-assembly and electro

[a] School of Chemistry and Chemical Engineering, South China University of Technology, Guangzhou, China.
[b] State Key Laboratory of Pulp and Paper Engineering, South China University of Technology, Guangzhou, China.
[c] Institute of Polymer Optoelectronic Materials and Devices, State Key Laboratory of Luminescent Materials and Devices, South China University of Technology, Guangzhou, China.
*Corresponding author. Email: celiy@scut.edu.cn and zhicaihe@scut.edu.cn

†Electronic Supplementary Information (ESI) available: [the results including SEM images of various block-like self-assemblies from LS and ALS; DLS measurement of LS solution and ALS solution in H_2O/EtOH (v/v, 1/3); Proposed schematic for the polymerization of EDOT in the presence of LS and ALS; UV absorption spectra of PEDOT:LS and PEDOT:ALS aqueous dispersion]. See DOI: 10.1039/x0xx00000x

transfer process during oxidation of LS, we proposed a study of the hole transport properties of LS and ALS. Based on the aggregation behaviour and electron transfer properties of LS and ALS, LS and ALS were used as dopants to disperse poly (3, 4-ethylene dioxythiophene) (PEDOT) for preparing the conductive polymers PEDOT:LS and PEDOT:ALS.

During the past decades of development of organic electronic devices including polymeric light emitting diodes (PLEDs), organic solar cells (OSCs) and organic photovoltaics (OPVs), interface modifier materials played indispensable roles for both anode and cathode.[19-24] It is an exciting result that a power conversion efficiency (PCE) exceeding 10% has been demonstrated in a highly efficient single junction PSCs with poly[(9,9-bis(3,-(N,N-dimethylamino) propyl)-2,7-fluorene)-alt-2,7-(9,9–dioctylfluorene)] (PFN) modified cathode.[25,26]

In contrast, for the modification of anode, poly (3, 4-ethylene dioxythiophene): poly (styrene sulfonic acid) (PEDOT:PSS) acts a hole transport material (HTM) and plays indispensable role as one of the most widely employed HTMs to modify indium-tin oxide (ITO) anode with good performances.[27] However, numerous alternative materials of PEDOT:PSS have been pursued because it is well known to corrode ITO at elevated temperatures due to its high acidity.[28] New solution-processable HTMs are still in demand and chemistry scientists have made great effort to explore new alternative materials.[29-36] Recently, we reported that PEDOT:SL as hole transporting material exhibited promising performance in polymer solar cells.[37] In order to study the effect of –OH and aggregation behaviour of lignosulfonate for the performance of PSCs, we choose LS and ALSs as starting materials in our previous manuscript[14] to study the effect in detail. The motivation for this is also in based on the following considerations.

Firstly, lignin,[38-40] the second most abundant plant resource, has three types of phenol derivatives including p-coumaryl alcohol, coniferyl alcohol, and sinapyl alcohol, which can be oxidized into radical or radical cation. Electron transfer process accompanied with the oxidation provide a potential for lignin to act as hole transport material. Traditional and classical hole transport/injection layer (HTL/HIL) poly-N-vinylcarbazole (PVK) contains electron-rich building block carbazole based derivative. However, there is rarely report of hole injection/transport layers based on the electron-rich compounds such phenol and its derivatives. It is well known that most of HTM will form radical cation during oxidation as shown in Scheme 1. PVK is one of the most widely studied HTM in previous work. It is noteworthy finding that the HOMO of PVK is -5.6 eV. We propose LS can act as HTM/HIT like PVK. The HOMO energy level of LS is also -5.6 eV and it is a potential good candidate as anode modifier. Secondly, the high acidity of PEDOT:PSS is from the anionic dispersant PSS, however, the limited sulfonation degree of LS and ALS will provide high pH for the dispersed conductive polymer, which will reduce its corrosion of ITO. Thirdly, as a water soluble polymer from biomass, lignosulfonate showed good dispersion properties in various industrial fields such as dimethomorph water-dispersible granule,[41] cement-water systems,[42] TiO_2 suspension[43] and coal water slurry in our group[14].

Scheme 1. The oxidation of PVK (a) and LS (b) as hole transport materials.

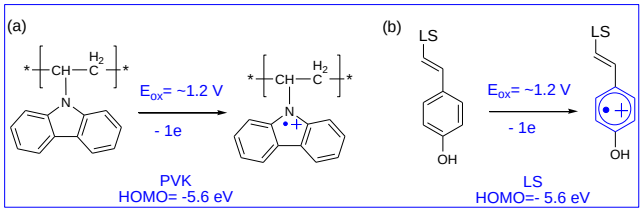

In the following report, We find LS and ALS could form unique block-like self-assembly in selective solvent. The aggregation behavior and formation mechanism was investigated in details. The block-like aggregates from A[illegible] were obviously larger than that from LS. It suggested that alkyl chain cross-linked polymerization of LS may lead to the intensive aggregation behavior of ALS. Furthermore, water soluble PEDOT:LS and PEDOT:ALS was prepared and applied as hole extraction layer in polymer solar cells (PSCs). The rusults indicated that the content of phenolic hydroxyl group (-OH) affect power conversion efficiency (PCE) of PSCs, and a PCE of 5.19% from PEDOT:LS-1:1 was achieved with device structure of ITO/HEL/PTB7:PC_{71}BM/Al. Our results showed LS might be of promising potential as dopant of semiconductors, such as PEDOT in organic electronics. The underlying mechanism was also studied and discussed in details.

Results and discussion

Aggregation behaviour of LS and ALS

To investigate the aggregation behaviour of LS and ALS, we are surprise to find that the unique block-like self-assembly was fabricated from LS and ALS in selective solvent for this study. The preparation was preceded as follow. LS was first dissolved

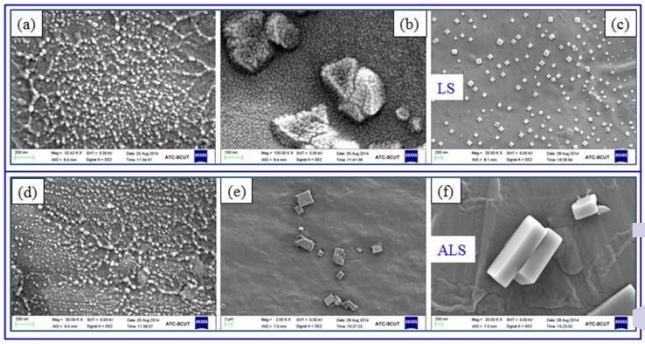

Fig.1. (a-c) The nano-size block-like aggregates from LS via self-assembly in first stage a, second stage b and third stage c. (d-f) The micro-size block-like aggregates from ALS via self-assembly in first stage d, second stage e and third stage f.

in water to prepare 0.2 mg mL^{-1} aqueous solution, followed by the addition of ethanol to achieve 0.05 mg mL^{-1} solution. The

ratio of H_2O/ethanol was 1/3. The mixture solution was stirred for 3 h and left at room temperature to obtain the unique block-like self-assembly. The detailed formation of the block-like aggregates structure at different stages was analysed using scanning electron microscope (SEM), transmission electron microscopy (TEM), Dynamic light scattering (DLS), X-ray photoelectron spectroscopy (XPS) andSmall-angle X-ray scattering (SAXS).

The novelty of this block-like aggregates formation mechanism emerges by comparison to other lignin nano- and micro- structures, which was investigated by SEM as shown in Fig. 1. It is well known that lignosulfonate exists as nano-size oval-shaped aggregates in dilute water solution.[14,15] As shown in Fig. 1(a,d), a lot of nano-aggregates were observed by SEM in the first stage. The diameter was appropriately ~20 nm. When the ethanol was added into the aqueous solution,thedegree of aggregation from LS and ALS is obviously different from each other. Structures consisted of many nano-aggregates yield block-like self-assembly was formed as shown in the second stage (Fig. 1 b,e). Finally, the homogeneous and unique block-like self-assembly was formed both from LS and ALS as shown in Fig. 1 (c,f). However, Block-like self-assemblies of nano-sizewere observed from LS, and that of micro-size were observed from ALS. Similar SEM images were also shown in Fig. S1. It suggested that alkyl chain cross-linked polymerization of LS may lead to the intensive aggregation behavior of ALS. Lignosulfonate, as an amorphous polymer, is an amphiphilic polymer with a lot of aromatic benzene ring, which is easy to aggregate in selective solventvia CH- π and π-π interaction to yield the unique self-assembly[44].

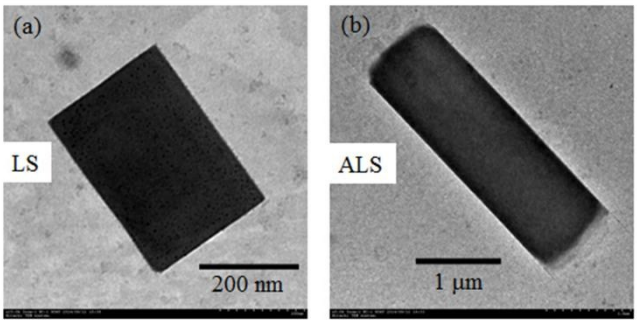

Fig.2. Typical TEM images of homogeneous nano-sized block-like self-assembly from LS (a) and micro-sized block-like self-assembly from ALS (b).

In order to investigate the formation mechanism of block-like self-assembly in more detail. TEM and DLS were conducted in this study. It was confirmed that LS could self-assemble into nano-sized block-like aggregate in H_2O/ethanol solution and ALS could form micro-sized block-like self-assembly as shown in Fig. 2. The block-like structure contained a lot of compacted nano-aggregates from LS and ALSseemed to behomogeneous and well-defined. Dynamic light scattering study of block-like aggregates can give important information about the solution self-assembly process. As shown in Fig. S2, the average diameter of the block-like aggregates from LS solution was about 300 nmand that from ALS solution was 9 μm,which was consistent with the electron microscopy results above. These results indicated that the block-like structure was formed via self-assembly in selective mixed solvents of water and ethanol and the aggregation degree of ALS is obviously serious compared with LS.

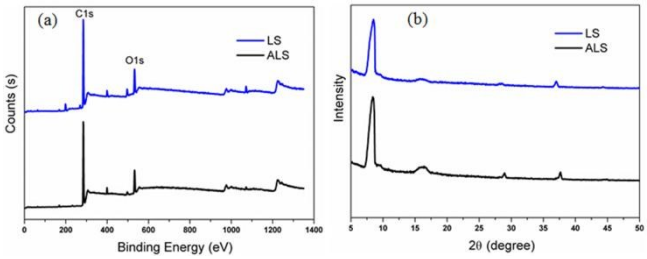

Fig.3. (a) X-ray photoelectron spectroscopy (XPS) of the block-like self-assemblies from LS and ALS on the same aluminum stubs with SEM. (b) Small-angle X-ray scattering (SAXS) patte of the block-like structure from LS and ALS.

X-ray photoelectron spectroscopy (XPS) measurement was conducted to test the element distribution of the block-like aggregates. As shown in Fig. 3a, high proportion of carbon and oxygen element was detected from the block-like structure, which further supported the above result that block-like self-assembly was formed from LS and ALS.

To determine the regular intrinsic characteristics of the block-like structure, small-angle X-ray scattering (SAXS) measurement was conducted by dropping the sample solution of block-like self-assembly on the silicon wafer and drying at room temperature. As shown in Fig. 3b, at low angles, strong reflections (8.1ºand 16.2 º) were detected by SAXS. All the above results indicated that the block-like structure h significant reflections. It is also further supported that the block-like self-assembly was fabricated from LS and ALS.

Electron transfer properties of LS and ALS

Based on the unique aggregation behaviour of ALS above, the electron transfer properties of ALS were also studied in our work, including electrochemical property and hole mobility measurement.

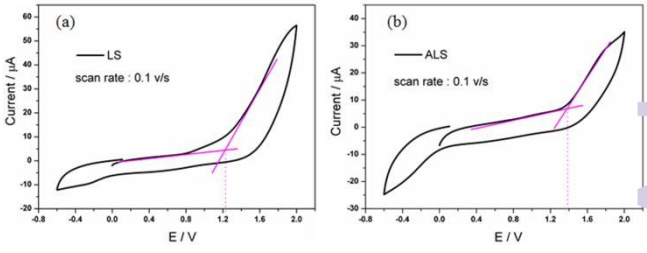

Fig.4. Cyclic voltammogram of LS and ALS film in 0.1 M Bu_4NPF_6 DCM solution.

Cyclic voltammogram (CV) were applied to study th oxidative activity of LS and ALS. The cyclic voltammogram of s and ALS film in 0.1 M Bu_4NPF_6 (in dichloromethane) solution

was used to investigate the electrochemical behaviour of LS and ALS as shown in Fig. 4. The oxidation peaks at 1.2 V and 1.4 V were observed at the LS and ALS modified electrode, respectively. It suggested that the oxidative activity of LS is better than that of ALS. The reaction mechanism for the reaction of LS and ALS at the surface of electrode was proposed, LS was proposed to be oxidized to form radical cation. Meanwhile, the phenolic hydroxyl group (-OH) of LS might be also oxidized into phenol radical. The –OH content of LS is more than that of ALS, which could lead to the better oxidative activity of LS.The electron transfer process provides a new concept for the design of HTM molecules.

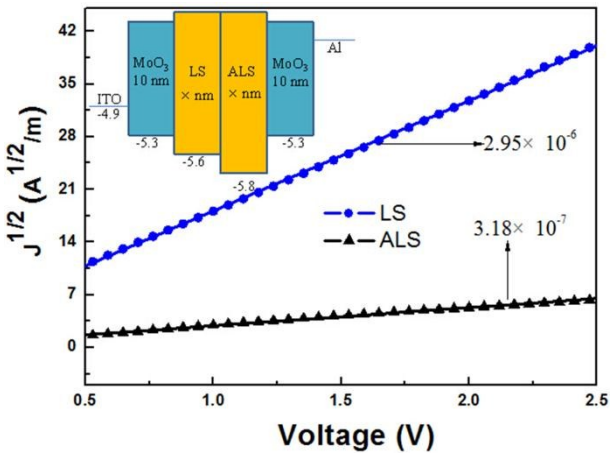

Fig.5.The J-V curves of hole-only devices with SCLC fitting from LS and ALS (the structure of hole-only devices inserted in the picture).

In order to make an quantitative evaluation on the hole transport property of LS and ALS materials, the hole mobility was measured by testing J-V characteristics of the hole-only devices with the device structure of ITO/MoO_3/Sample/MoO_3/Al as shown in the structure diagram inserted in Fig. 5. As a wide band gap semiconductor, MoO_3 is used to assist the holes transport to ITO anode and block the electrons injected from Al cathode at the same time. The observed dark current-voltage curve was then fitted by using the space-charge-limited current(SCLC) model, which is described by the equation as following:

$$J=(9/8)\varepsilon_r\varepsilon_0\mu(V^2/d^3)$$

In the equation above, ε_0 is the dielectric permittivity of free space, ε_r is the relative permittivity of the sample, μ is the mobility, and d is the thickness of sample. Thehole mobility value was obtained by SCLC equation with the detailed data listed in Fig. 5 and Table 1.

As can be seen from Fig5 and Table 1,the hole mobility of 2.95×10^{-6}cm^2 V^{-1} s^{-1}, estimated fromLS, is nearly one order of magnitude higher than that of ASL (3.18×10^{-7}cm^2 V^{-1} s^{-1}). The result indicates that the LS and ALS are potential water soluble organic semiconductor with hole transporting properties. Moreover, LS with more phenolic group content, has higher hole mobility than ASL with less phenolic group content. It suggested that phenolic group is conducive to the hole transporting property, which was in good agreement with the result of electrochemical property above.

Table 1. The hole mobilities of samples from SL and ASLs.

Samples	Thickness (L) (nm)	Slope (ρ)	Hole-mobility (cm^2 V^{-1} s^{-1})
LS	35	13.86	2.95×10^{-6}
ALS	50	2.45	3.18×10^{-7}

Dispersion of PEDOT and its application in polymer solar cells

Based on the unique aggregation behaviour and hole mobility of LS and ALS, LS and ALS was applied to disperse conductive polymer PEDOT and prepare PEDOT:LS and PEDOT:ALS aqueous dispersion, which was applied as hole extraction layer in polymer solar cells devices. The schematic for the polymerization of EDOT in the presence of LS and AL templates was proposed as shown in Fig 6.

UV-vis absorption spectra of PEDOT:LS and PEDOT:ALS aqueous dispersion were shown in Fig. S3. Because of higher phenolic hydroxyl group content of LS, the absorption intensity of PEDOT:LS from 250 to 300 nm is obviously stronger than that of PEDOT:ALS. The UV spectra of PEDOT:LS and PEDOT:ALS aqueous dispersion showed the presence of a biopolaron absorption band at 800 nm, which was ascribed to the π-π transition in the PEDOT polymer chain.[45] The broad absorption from 600 to 900 nm was also detected in both of PEDOT:LS and PEDOT:ALS aqueous dispersion. It further confirmed PEDOT:LS and PEDOT:ALS was successfully prepared in our study.

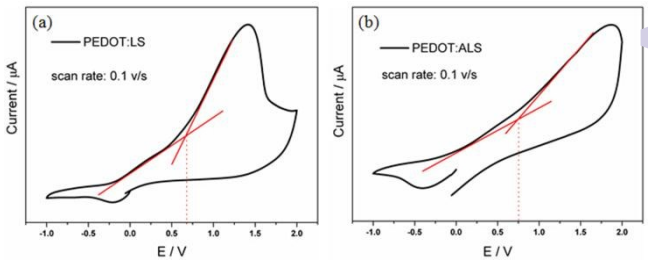

Fig.6. Cyclic voltammogram of PEDOT:LS film and PEDOT:ALS film in 0.1 M Bu_4NPF_6 DCM solution.

The cyclic voltammogram of PEDOT:LS film and PEDOT:ALS film in 0.1 M Bu_4NPF_6 (in dichloromethane) solution was also measured as shown in Fig. 6. Compared with that of PEDOT:ALS, An obvious oxidation peak at 0.65 V was observed at the PEDOT:LS modified electrode. Two oxidation potentials at 0.65 V and 0.75 V were observed at the PEDOT:LS and PEDOT:ALS modified electrode, respectively. The HOMO value of PEDOT:LS and PEDOT:ALS were calculated as -5.05 eV and -5.15 eV, respectively. It indicated LS has positive effect on conductive polymer PEDOT and LS with higher –OH content facilitate hole transfer of PEDOT:LS. The responding oxidation mechanism was proposed as shown in Fig. 7. It encourages us to study its potential application in organic electronics.

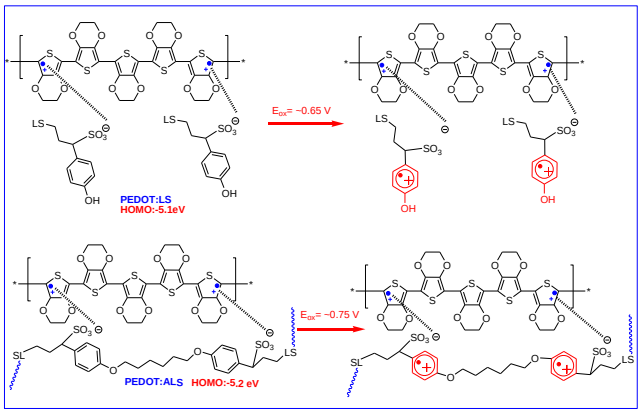

Fig.7. Proposed electron transfer process of PEDOT:LS (up) and PEDOT:ALS (down).

To evaluate the hole transport performance of PEDOT:LS and PEDOT:ALS, PSCs with PEDOT:LS and PEDOT:ALS as anode modifier were fabricated. The detailed device architecture of the PSCs and current density (J)-voltage (V) curves of the PSCs with different HTMs are shown in Fig. 8. The power conversion efficiency (PCE), short-circuit current density (J_{SC}), open-circuit voltage (V_{OC}) and fill factor (FF) of the PSCs are given in Table 2. PEDOT only showed a bad PCE of 2.91% with a FF of 48.04%. The same devices (ITO/HEL/PTB7:PC71BM/Al) with PEDOT:PSS modified anode showed a J_{SC} of 12.77, V_{OC} of 0.72 and PCE of 4.28% with a FF of 46.40% as shown in reference[46]. The PCE of

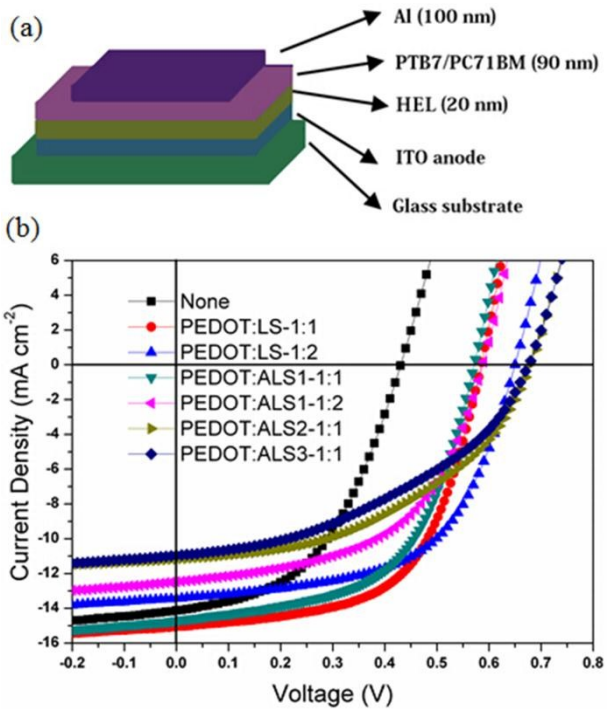

Fig.8. (a) Device architecture of the polymer solar cell (PSC). (b) J-V curves of PSCs with PEDOT only, PEDOT:LS and PEDOT:ALSs with different mass ratio in devices of ITO/HTM/PTB7:PC_{71}BM/Al.

the PSCs in a conventional device structure ITO/PEDOT:PSS/PTB7:PC_{71}BM/Al was 4.50% as another literatures reported[47] shown in Table 2. The PCEs of device with PEDOT:LS and PEDOT:ALSs with different mass ratio in a device structure ITO/PEDOT:PSS/PTB7:PC_{71}BM/Al were all investigated in our study as shown in Table 2. In previous manuscript,[14] the content of –OH decreased gradually from LS to ALS3. As can be seen from Table 2, the PCEs of the device with PEDOT:LS-1:1, PEDOT:ALS1-1:1, PEDOT:ALS2-1:1 and PEDOT:ALS3-1:1 were 5.19%, 4.75%, 3.49% and 3.11%, respectively. The PCEs decreased with the decrease of –OH content, which indicated that –OH is important for the electron transfer process. The results were consistent with the results of CV and hole mobility. In addition, when the mass ratio of PEDOT:LS and PEDOT:ALS1 was 1:2, the PCEs of device with PEDOT:LS-1:2 and PEDOT:ALS-1:2 were 5.02% and 3.73% which were lower than that of device using PEDOT:LS-1:1 and PEDOT:ALS-1:1. It is noteworthy that PEDOT:LS-1:1 was applied, a PCE of 5.19% with J_{SC} of 15.06 mA cm^{-1}, V_{OC} of 0.58 V and FF of 58.87 % was obtained. The PCE of PEDOT:LS-1:1 (5.19%) was higher than that of PEDOT:PSS[46] (4.50%). The results indicate that LS might be of promising potential as dopant in semiconductors. It encourages us to study its potential further in future. We proposed the possible mechanism based the following three aspects.

Table 2. Photovoltaic Performances of PSCs with PEDOT:PSS, PEDOT:LS and PEDOT:ALS with different proportionin devices of ITO/HTM/PTB7:PC_{71}BM/Al.

anode	V_{OC}(V)	J_{SC}(ma cm^{-2})	FF(%)	PCE(%)
PEDOT:PSS[46]	0.72	12.77	46.40	4.28
PEDOT:PSS[47]	0.62	14.58	50.00	4.50
None	0.43	14.12	48.04	2.91
PEDOT:LS-1:1	0.58	15.06	58.87	5.19
PEDOT:LS-1:2	0.65	13.43	57.55	5.02
PEDOT:ALS1-1:1	0.57	14.69	56.40	4.75
PEDOT:ALS1-1:2	0.56	12.20	54.55	3.73
PEDOT:ALS2-1:1	0.68	11.17	45.88	3.49
PEDOT:ALS3-1:1	0.68	10.96	41.74	3.11

On one hand, from the electrochemical property and hole mobility of LS and ALS, both of LS and ALS might play as semiconductor for hole collection in PSCs. However, hole mobility of ALS was much lower than that of LS which suggested that phenolic group content could affect the hole transporting property. Combined with the unique aggregation behaviour, aggregation degree of ALS is obviously serious compared with LS. LS and ALS were applied as a novel and potential hole extraction layer (HEL) in polymer solar cells.

On the other hand, in our work, alkyl chain was introduced in phenolic group of LS to obtain ALSs, the results above indicated that phenolic group content could affect the hole transporting property and electron transfer property shown in Fig.4 and Fig. 5. The oxidation process of PEDOT:LS and PEDOT:ALS were also investigated in our study as shown in Fig. 6. As can be seen in Fig. 9, the HOMO energy level values were 5.0 eV, 5.05 eV and 5.15 eV for PEDOT:PSS, PEDOT:LS and PEDOT:ALS, respectively, which suggested that it has small

energy gaps in thin film for PEDOT:LS compared to PEDOT:ALS. This is very important for hole to transport. Therefore, PEDOT:LS exhibited better power conversion efficiency than PEDOT:ALS acting as HEL in polymer solar cells.

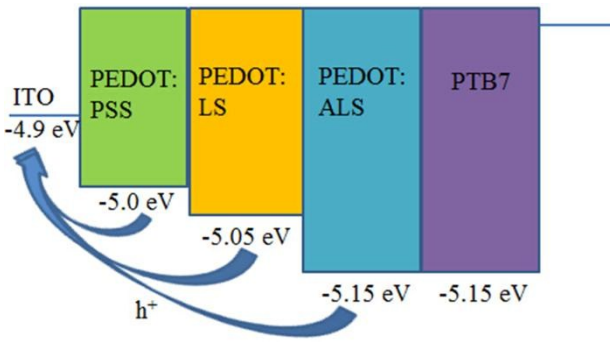

Fig.9. HOMO energy levels of ITO, PEDOT, PEDOT:LS, PEDOT:ALS and PTB7 (HOMO of PEDOT:LS and PEDOT:ALS were calculated as -5.05 eV and -5.15 eV, respectively, as shown in Fig. 6).

Finally, as studied previously, ALS polymer is easier than LS to aggregate, especially to fabricate unique block-like aggregates with micro-size in selective solvent. The aggregation behavior also affects the hole transporting property of conductive PEDOT. Therefore, we studied the surface morphologies of PEDOT:LS film and PEDOT:ALS by AFM as shown in Fig. 10a-f. There is significant difference between them. Overall, the AFM images of PEDOT:ALS films were rough, which was ascribed to the intensive aggregation capability of ALS polymer. The AFM images of PEDOT:LS films were more homogeneous and compacted than that of PEDOT:ALS films. The particle size of PEDOT:LS was also relatively smaller than that of

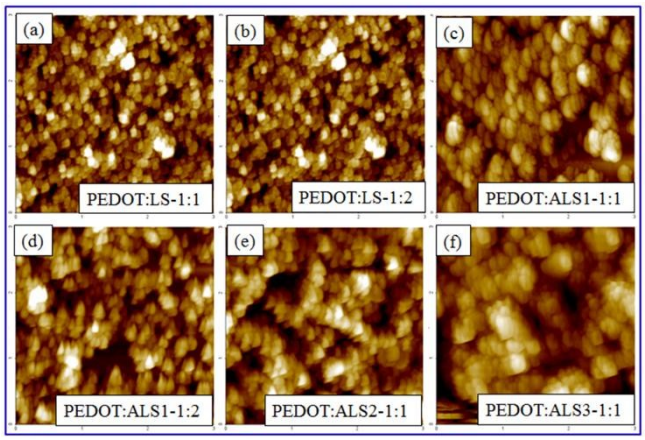

Fig.10. AFM images of PEDOT:LS films with different mass ratio (a,b) , PEDOT:ALS films with different mass ratio (c,d) and PEDOT:ALS2 film (e), PEDOT:ALS3 film (f). The size of the images is 3 μm×3 μm.

PEDOT:ALS. In the above results, the more homogeneous and smaller size compact nano-aggregates might facilitate charge transport of PEDOT:LS polymers in film. It is an interesting result that LS can act as dopant of PEDOT even it has so complex, disordered and amorphous structure. Comparing with PSS with regular structure, the stronger crystallization character and oxidation behaviors of LS might contributed the unexpected hole transport of PEDOT:LS film. Moreover, the pH value of PEDOT:ALS aqueous dispersion (pH 3.9) was higher than that of PEDOT:PSS (pH 1.9), which is conducive to reduce the corrosion of ITO during device operation.

All in one word, based on the unique aggregation behavior, eletron transfer property and hole mobility of LS compared with ALS polymer, LS showed a novel application potential as dopant for water soluble polymeric semiconductor. PEDOT:LS showed promising performance as hole-transport material in polymer solar cells (PSCs), which is comparable with that of conversional PEDOT:PSS. The results have rarely reported, to date. LS, as a novel hole transport material from renewable bioresource, might be a potential water soluble polymeric semiconductor. The dopant design concept of PEDOT provides a promising strategy to develop stable water soluble PEDOT semiconductive polymer which will accelerate the commercialization of solution processable organic electronics in future.

Conclusions

To summarize, the aggregation behaviour of LS and ALS was investigated and block-like structures were obtained via self-assembly with complex three-dimensional amorphous structure for the first time. The block-like self-assemblies from LS and ALS may lead to create a novel class of multifunctional materials. The size of block-like aggregates from ALS (micro-size) is obviously bigger than that from LS (nano-size), which was ascribed to the high molecular weight of ALS. We studied hole transport property of LS and ALS with space-charge-limited current method (SCLC). The average hole mobilities of 2.95×10^{-6} and 3.18×10^{-7} cm^2 V^{-1} s^{-1} were estimated for LS and ALS, which indicated that LS and ALS are potential water soluble polymeric p-type semiconductors and phenolic group content could affect the hole transporting property. All of results of CV and hole mobility indicate that LS could be applied as a novel hole transport material for organic electronics. On the basis of the unique aggregation behaviour and hole mobility of LS and ALS, water soluble PEDOT:LS and PEDOT:ALS were all prepared and applied as hole extraction layer in polymer solar cells. The PCEs decreased with the decrease of –OH content, which indicated that –OH is important for the electron transfer process. The results were consistent with the results of CV and hole mobility. Moreover, the power conversion efficiencies (PCE) of 5.19 % was achieved in devices of ITO/HTM/PTB7:PC_{71}BM/Al, which was higher than that of PEDOT:PSS[46,47] (PCE 4.28% and 4.50%). Moreover, PEDOT:LS might exhibit potential application in various fields including perovskite-based solar cells[48-53] and hybrid solar cells[54-59]. Our results showed LS might be of promising potential as dopant of semi-conductive polymers such as PEDOT in organic electronics, as alternative candidate of PSS which is non-conjugated. We believe the device performance will be further improved when better HTM based on phenol derivatives are found. More importantly, this work provides a concept for the design of hole transport materials

containing polyaromatic hydrocarbons[60-66] and also a novel perspective for high value-added application of lignin, a cheap and renewable biomass.

Experimental Section

Materials

LS was supplied by the Quanlin paper mill (Shandong province,China). ALS was prepared from alky chain-coupled polymerization of LS in our lab. All other chemicals were of analytical grade.

Aggregation behaviour and hole mobility

Scanning electron micrographs (SEM) were recorded with a Nova Nano SEM instrument (Zeiss, Netherlands). Samples were mounted on aluminum stubs by means of double-sided conductive adhesive and sputtered with Au/Pd to reduce charging effects.

Atomic force microscope (AFM) images were observed using Park XE-100 instrument by tapping mode. The AFM samples were prepared by dropping the sample solution on the substrate as slow as possible and drying under room temperature for 24 hours.

Transmission electron microscopy (TEM) images were obtained using a HITACHI H-7650 electron microscope with an accelerating voltage of 200 kV. The TEM samples were prepared by dropping diluted sample solution onto the copper grids coated with a thin carbon film.

Dynamic light scattering (DLS) experiments were performed on Zeta PALS instrument (Brookhaver, America). The concentration of samples was 0.05 mg mL^{-1} in H_2O/Ethanol (v/v, 1:3) at around pH 7.0.

The block-like self-assemblies for X-ray photoelectron spectroscopy (XPS) were prepared by dropping the samples solution on tinfoil and drying naturally under room temperature.

The block-like self-assemblies for small-angle X-ray scattering (SAXS) were prepared by dropping the samples solution on Si substrate and drying naturally under room temperature.

Cyclic voltammetry measurement was conducted as follows: a glassy carbon electrode was first polished carefully with alumina powder to a mirror finish surface and rinsed with distilled water repetitively. LS and ALS solution were prepared by dissolving 10 mg sample in 1 mL distilled water. Then sample film was deposited at the surface of the clean glassy carbon electrode. PEDOT:LS and PEDOT:ALS film was directly deposited at the surface of the clean glassy carbon electrode. The resulting electrode was immersed in 0.1 M Bu_4NPF_6 DCM solutions, and was stabilized in 0.1 M Bu_4NPF_6 DCM solutions by scanning the potential between -0.6 and +2.0 V at a scan rate of 100 mV s^{-1}.

The hole mobilities of LS and ALS were measured using space-charge-limited current (SCLC) method by testing J-V characteristics of hole-only device structure: ITO/MoO_3 (10 nm)/Sample/MoO_3 (10 nm)/Al (100 nm). The film of sample was spin-coated with concentration of 80 mg mL^{-1} and the solvent of sample is deionized water.

Dispersion of PEDOT and application in polymer solar cells

Preparation of PEDOT:LS and PEDOT: ALS: a proposed schematic for the polymerization of EDOT in the presence of LS and ALS dispersant is shown in Fig. 6. The preparation was as follows. Sample (LS or ALS) (1 g and 2 g, respectively) was dissolved in 200 mL of distilled water, then 1 g EDOT monomer was added with slow stirring speed for 10 min and the pH value of the solution was adjusted to 2. To the mixed solution, 1.93 g of oxidant ammonium persulfate (APS) solution was added slowly under high speed stirring. The reaction was kept at room temperature for 24 hours, and dialyzed to remove inorganic salt. The dialysis product was used for detection through ultrasonication for 10 min. The UV-vis absorption spectra of PEDOT:LS and PEDOT:ALS aqueous dispersion were measured using Shimadzu UV-3600 spectrophotometer (Japan).

Fabrication and characterization of OPVs: ITO-coated glass substrates were cleaned by sonication in acetone, detergent, deionized water, and isopropyl alcohol and dried in a nitrogen stream, followed by an oxygen plasma treatment. In order to fabricate photovoltaic devices, a thin hole-transportation layer (ca. 40 nm) of PEDOT:SL and PEDOT:ALS (filtered at 0.45 μm) was spin-cast on the pre-cleaned ITO-coated glass substrates and baked at 120 ℃ for 20 min under ambient conditions. The active layer PTB7:$PC_{71}BM$ (10:15 mg mL^{-1}) was prepared by spin-casting chlorobenzene solution with the addition of a small amount of DIO (CB: DIO = 100:3, V/V) at 1500 rpm for 30 s in dry box. The thickness of the PTB7:$PC_{71}BM$ layer was about 100 nm. 4 h later, methanol was spin-coated on the active layer at 2000 rpm for 30 s. The Al electrode were thermally deposited for 100 nm through a mask in vacuum (<5 × 10^{-4} Pa). All steps except processing of HTMs were performed in the glove box. The effective device area was about 0.16 cm^2. The current density–voltage (J–V) characteristics were measured using a Keithley 2400 source meter. The photovoltaic devices were characterized using a calibrated AM1.5 G solar simulator (Oriel model 91192), under light intensity of 100 mW cm^{-2}.

Acknowledgements

The authors would like to acknowledge the financial support of National Natural Science Foundation of China (21402054, 21436004), National Basic Research Program of China 973 (2012CB215302), International S&T Cooperation Program of China (2013DFA41670).

Notes and references

1 S. H. Im, U. Y. Jeong and Y. N. Xia. *Nat. Mater.,* 2005, **4**, 671.
2 D. H. Kim, J. T. Han, Y. D. Park, Y. Jang, J. H. Cho, M. Hwang and K. Cho. *Adv. Mater.,* 2006, **18**, 719.
3 T. Jiang, C. F. Xu, X. B. Zuo and V. P. Conticello. *Angew. Chem. Int. Edit.,* 2014, **53**, 8367.
4 J. Zhang, X. F. Chen, H. B. Wei and X. H. Wan. *Chem. Soc. Rev.,* 2013, **42**, 9127.
5 J. Z. Du and R. K. O'Reilly. *Soft Matter,* 2009, **5**, 3544.
6 O. Ikkala and G. ten Brinke. *Science,* 2002, **295**, 2407.
7 A. H. Groschel, A. Walther, T. I. Lobling, F. H. Schacher, H. Schmalz and A. H. E. Muller. *Nature,* 2013, **503**, 247.
8 X. Y. Yang, A. Leonard, A. Lemaire, G. Tian and B. L. Su. *Chem. Commun.,* 2011, **47**, 2763.

9 V. Percec, M. Glodde, T. K. Bera, Y. Miura, I. Shiyanovskaya, K. D. Singer, V. S. K. Balagurusamy, P. A. Heiney, I. Schnell, A. Rapp, H. W. Spiess, S. D. Hudson and H.Duan.*Nature,*2002, **419**, 384.
10 A. Ajayaghosh and V. K. Praveen. *Accounts Chem. Res.,* 2007, **40**, 644.
11 D. L. Wang, G. S. Tong, R. J. Dong, Y. F. Zhou, J. Shen and X. Y. Zhu. *Chem. Commun.,* 2014, **50**, 11994.
12 X. T. Zhang, C. Y. Li and Y. J. Luo. *Langmuir,* 2011, **27**, 1915.
13 S. T. Sun and P. Y. Wu. *Soft Matter,* 2011, **7**, 7526.
14 N. L. Hong, Y. Li, W. M. Zeng, M. K. Zhang, X. W. Peng and X. Q. Qiu. *RSC Adv.,* 2015, **5**, 21588.
15 X. Q. Qiu, Q. Kong, M. S. Zhou and D. J. Yang. *J. Phys. Chem. B.* 2010, **114**, 15857.
16 C. Steelink, J. D. Fitzpatrick, L. D. Kispert and J. S. Hyde. *J. Am. Chem. Soc.,* 1968, **90**, 4354.
17 C. A. Steelink. *Tetrahedron Lett.,* 1966, **7**, 105.
18 H. Sato and F. P. Guengerich. *J. Am. Chem. Soc.,* 2000, **122**, 8099.
19 C. W. Tang, S. A. VanSlyke and C. H. Chen. *J. Appl. Phys.,* 1989, **65**, 3610.
20 Q. L. Huang, G. A. Evmenenko, P. Dutta, P. Lee, N. R. Armstrong and T. J. Marks. *J. Am. Chem. Soc.,* 2005, **127**, 10227.
21 P. Kundu, K. R. J. Thomas, J. T. Lin, Y. T. Tao and C. H. Chien. *Adv. Funct. Mater.,* 2003, **13**, 445.
22 G. Teran-Escobar, J. Pampel, J. M. Caicedo and M. Lira-Cantu. *Energy Environ. Sci.,* 2013, **6**, 3088.
23 X. Y. Cheng, Y. Y. Noh, J. P. Wang, M. Tello, J. Frisch, R. P. Blum, A. Vollmer, J. P. Rabe, N. Koch and H. Sirringhaus. *Adv. Funct. Mater.,* 2009, **19**, 2407.
24 L. Chen, C. Xie and Y. W. Chen. *Adv. Funct. Mater.,* 2014, **24**, 3986.
25 Z. C. He, C. M. Zhong, S. J. Su, M. Xu, H. B. Wu and Y. Cao. *Nat. Photonics,* 2012, **6**, 591.
26 Z. C. He, B. Xiao, F. Liu, H. B. Wu, Y. L. Yang, S. Xiao, C. Wang, T. P. Russell and Y. Cao. *Nat. Photonics,* 2015, **9**, 174.
27 W. F. Zhang, B. F. Zhao, Z. C. He, X. M. Zhao, H. T. Wang, S. F. Yang, H. B. Wu and Y. Cao. *Energ. Environ. Sci.,* 2013, **16**, 1956.
28 S. K. Hau, H. L. Yip, N. S. Baek, J. Y. Zou, K. O'Malley and A. K. Y. Jen. *Appl. Phys. Lett.,* 2008, **92**, 253301.
29 S. D. Collins, C. Luo, G. C. Bazan, T. Q. Nguyen and A. J. Heeger, *Adv. Mater.,* 2013, **25**, 1646.
30 J. Shao, W. Y. Tan, Q. D. Li, X. Song, Y. H. Li, G. Liu, Y. Q. Mo, X. H. Zhu, J. B. Peng and Y.Cao.*Org. Electron.,* 2013, **14**, 2051.
31 E. L. Ratcliff, A. Garcia, S. A. Paniagua, S. R. Cowan, A. J. Giordano, D. S. Ginley, S. R. Marder, J. J. Berry and D. C. Olson. *Adv. Energy Mater.,* 2013, **3**, 647.
32 Z. W. Wu, S. Bai, J. Xiang, Z. C. Yuan, Y. G. Yang, W. Cui, X. Y. Gao, Z. Liu, Y. Z. Jin and B. Q. Sun. *Nanoscale,* 2014, **6**, 10505.
33 J. H. Kim, P. W. Liang, S. T. Williams, N. Cho, C. C. Chueh, M. S. Glaz, D. S. Ginger and A. K. Y. Jen.*Adv. Mater.,* 2015, **27**, 695.
34 C. E. Tsai, M. H. Liao, Y. L. Chen, S. W. Cheng, Y. Y. Lai, Y. J. Cheng and C. S. Hsu. *J. Mater. Chem. A.,* 2015, **3**, 6158.
35 Y. Wei, P. J. Liu, R. H. Lee and C. P. Chen. *RSC Adv.,* 2015, **5**, 7897.
36 X. D. Li, X. H. Liu, X. Y. Wang, L. X. Zhao, T. G. Jiu and J. F. Fang. *J. Mater. Chem. A.,* 2015, **3**, 15024.
37 Y. Li and N. L. Hong. *J. Mater. Chem. A.,* 2015, DOI: 10.1039/C5TA05167C.
38 W. Boerjan, J. Ralph and M. Baucher. *Annu. Rev. Plant Biol.,* 2003, **54**, 519.
39 J. Zakzeski, P. C. A. Bruijnincx, A. L. Jongerius and B. M. Weckhuysen. *Chem. Rev.,* 2010, **110**, 3552.
40 C. P. Xu, R. A. D. Arancon, J. Labidi and R. Luque. *Chem. Soc. Rev.,* 2014, **43**, 7485.
41 Z. L. Li, Y. X. Pang, H. M. Lou and X. Q. Qiu. *Bioresources,* 2009, **4**, 589.
42 H. M. Lou, H. R. Lai, M. X. Wang, Y. X. Pang, D. J. Yang, X. Q. Qiu, B. Wang and H.B. Zhang. *Ind. Eng. Chem. Res.,* 2013, **52**, 16101.
43 H. F. Zhou, D. J. Yang, X. Q. Qiu, X. L. Wu and Y. Li. *Appl. Microbiol. Biotechnol.,* 2013, **97**, 10309.
44 Y. J. Zheng, H. X. Zhou, D. A. Liu, G. Floudas, M. Wagner, K. Koynov, M. Mezger, H. J. Butt and T. Ikeda. *Angew. Chem. Int Edit.,* 2013, **52**, 4845.
45 J. Ouyang, Q. F. Xu, C. W. Chu, Y. Yang, G. Li and J. Shinar, *Polymer,* 2004, **45**, 8443.
46 M. V. Srinivasan, M. Ito, P. Kumar, K. Abhirami, N. Tsuda, J. Yamada, P. K. Shin and S. Ochiai. *Ind. Eng. Chem. Res.,* 2015, **54**, 181.
47 S. Guo, B. Y. Cao, W. J. Wang, J. F. Moulin and P. Muller-Buschbaum, *ACS Appl. Mater. Inter.,* 2015, **7**, 4641.
48 W. S. Yang, J. H. Noh, N. J. Jeon, Y. C. Kim, S. Ryu, J. Seo and S. I. Seok, *Science,* 2015, **348**, 1234.
49 W. Ke, G. Fang, Q. Liu, L. Xiong, P. Qin, H. Tao, J. Wang, H. Lei, B. Li, J. Wan, H. Lei, B. Li, J. Wan, G. Yang and Y. Yan, *J. Am. Chem. Soc.,* 2015, **137**, 6730.
50 N. J. Jeon, J. H. Noh, W. S. Yang, Y. C. Kim, S. Ryu, J. Seo and S. I. Seok, *Nature,* 2015, **517**, 476.
51 M. Z. Liu, M. B. Johnston and H. J. Snaith, *Nature,* 2013, **501**, 395.
52 H. P. Zhou, Q. Chen, G. Li, S. Luo, T. B. Song, H. S. Duan, Z. R. Hong, J. B. You, Y. S. Liu and Y. Yang, *Science,* 2014, **345**, 542.
53 M. He, D. J. Zheng, M. Y. Wang, C. J. Lin and Z. Q. Lin, *J. Mater. Chem. A.,* 2014, **2**, 5994.
54 M. M. Lee, J. Teuscher, T. Miyasaka, T. N. Murakami and H. J. Snaith, *Science,* 2012, **338**, 643.
55 W. J. E. Beek, M. M. Wienk and R. A. J. Janssen, *Adv. Mater.,* 2004, **16**, 1009.
56 J. H. Heo, S. H. Im, J. H. Noh, T. N. Mandal, C. S. Lim, J. A. Chang, Y. H. Lee, H. J. Kim, A. Sarkar, M. K. Nazeeruddin, M. Gratzel and S. I. Seok, *Nat. Photonics,* 2013, **7**, 487.
57 S. D. Oosterhout, M. M. Wienk, S. S. van Bavel, R. Thiedmann, L. J. A. Koster, J. Gilot, J. Loos, V. Schmidt and R. A. J. Janssen, Nat. Mater., 2009, 8, 818.
58 J. P. Thomas, L. Y. Zhao, D. McGillivray and K. T. Leung, *J. Mater. Chem. A.,* 2014, **2**, 2383.
59 J. P. Thomas and K. T. Leung, *Adv. Funct. Mater.,* 2014, **24**, 4978.
60 A. K. Sangha, J. M. Parks, R. F. Standaert, A. Ziebell, M. Davis and J. C. Smith, *J. Phys. Chem. B,* 2012, **116**, 4760.
61 G. Milczarek and O. Inganas, Science, 2012, 335, 1468.
62 Y. Li, W. K. Heng, B. S. Lee, N. Aratani, J. L. Zafra, N. Bao, R. Lee, Y. M. Sung, Z. Sun, K. W. Huang, R. D. Webster, J. T. L. Navarrete, D. Kim, A. Osuka, J. Casado, J. Ding and J. S. Wu, *J. Am. Chem. Soc.,* 2012, **134**, 14913.
63 Y. Li, K. W. Huang, Z. Sun, R. D. Webster, Z. B. Zeng, W. D. Zeng, C. Y. Chi, K. Furukawa and J. S. Wu, *Chem. Sci.,* 2014, **5**, 1908.
64 M. Abe, *Chem. Rev.,* 2013, **113**, 7011.
65 T. Aotake, M. Suzuki, N. Aratani, J. Yuasa, D. Kuzuhara, H. Hayashi, H. Nakano, T. Kawai, J. S. Wu and H. Yamada, *Chem. Commun.,* 2015, **51**, 6734.
66 W. D. Zeng, B. S. Lee, Y. M. Sung, K. W. Huang, Y. Li, D. Kim and J. S. Wu, *Chem. Commun.,* 2012, 48, 7684.

Table of Contents (TOC)

Aggregation behaviour and –OH content of lignosulfonate play key role for the promising performance while PEDOT:LS acts as HEL in PSCs.